INFLUENCE OF THE BUBBLER TEMPERATURE ON PSG AND EMITTER FORMATION DURING POCL₃ DIFFUSION PROCESS

M. Steyer[1], A. Dastgheib-Shirazi[1], G. Micard[1], H. Wagner[2,3], P.P. Altermatt[2], G. Hahn[1]

[1]Department of Physics, University of Konstanz, 78457 Konstanz, Germany
[2]Dep. Solar Energy, Inst. Solid-State Physics, Leibniz University of Hannover, 30167 Hannover, Germany
[3]Massachusetts Institute of Technology, Cambridge, MA 02139, USA
Author for correspondence: michael.steyer@uni-konstanz.de Tel.: +49 7531 882081, Fax: +49 7531 883895

ABSTRACT: In this work we focus on the emitter formation and its dopant source, the PhosphoSilicate Glass (PSG), formed by POCl₃ diffusion. An optimum emitter requires an exact adjustment of diffusion parameters, such as process temperature, time, POCl₃-N₂ gas flow and O₂ gas flow. Another important process parameter which is normally kept constant but also has a strong influence on PSG and emitter formation, is the temperature of the POCl₃ bubbler. We characterise PSG and emitter in dependence of the bubbler temperature, within a temperature range from 15.5°C to 24.5°C. PSG thickness varies in respect to bubbler temperature from 29 nm to 33 nm, which is a remarkably narrow range. Further, the total amount of phosphorus in the PSG is measured using ICP-OES. By combination of measured PSG thickness and its P dose, we determine a lower limit for P concentration in the PSG for different bubbler temperatures. On the other hand, the emitter is characterised by the active doping profile, measured by ECV. The plateau depth of these profiles depend clearly on the bubbler temperature. In addition, we show the influence of bubbler temperature on the emitter saturation current density. Finally, the effect of the bubbler temperature has been transferred to industrial screen-printed 6-inch solar cells.
Keywords: POCl₃, Diffusion, Emitter, PSG, Bubbler temperature

1 INTRODUCTION

An n-type emitter is most commonly formed by POCl₃ diffusion process. The diffusion process is divided in the pre-deposition step, where a dopant layer is formed, and a drive-in step. During pre-deposition, liquid POCl₃ from the bubbler is transported by N₂ carrier gas into the diffusion tube. Combined with a gas flow of O₂, the formation of phosphorus pentoxide (P₂O₅) is expected:

$$4POCl_3 + 3O_2 \rightarrow 2P_2O_5 + 6Cl_2 \qquad (1)$$
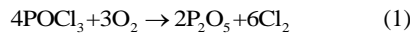
Subsequently, the P₂O₅ reacts with silicon to silica (SiO₂) and atomic phosphorus diffuses into the silicon wafer. SiO₂ along with P₂O₅ forms the phosphosilicate glass layer, which acts as a dopant source during the diffusion process for emitter formation:

$$2P_2O_5 + 5Si \rightarrow 5SiO_2 + 4P \qquad (2)$$
$$SiO_2 + P_2O_5 \rightarrow P_2O_5 \cdot SiO_2 \qquad (3)$$
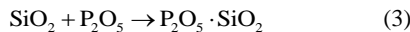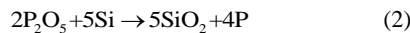
After the pre-deposition phase the drive-in step follows, where the POCl₃-N₂ gas flow is turned off and phosphorus is driven in further into the silicon wafer.

The PSG growth and thus the emitter formation depend on several diffusion parameters, such as process temperature, time, POCl₃-N₂ gas flow and O₂ gas flow. An additional parameter, which is usually untouched, is the temperature of the liquid POCl₃ bubbler. A change of the bubbler temperature has a strong effect on the transported amount of POCl₃ to the diffusion tube and so on PSG and emitter formation. Normally the amount of POCl₃ in the diffusion tube can be adjusted by the flow of the carrier gas. In case the bubbler temperature is varied, the carrier gas flow is kept constant and so strong influences on phosphorus precipitate formation and homogeneity during the diffusion process are possible.

In the following, we investigate the influence of the bubbler temperature systematically. The results will help to improve the understanding of PSG growth and emitter formation. In particular, the experimental data can be used to improve existing models of phosphorus diffusion [1-2] by including the PSG growth behaviour and its composition [3-5].

2 EXPERIMENTAL SET-UP

The standard base material is p-type, 6-inch Cz silicon wafers with a bulk resistivity of 2.7 Ωcm. Additionally, we use p-type, 5x5 cm² FZ silicon wafers with a bulk resistivity of 2 Ωcm and 200 Ωcm. Sample preparation for PSG and emitter characterization is indicated in Fig. 1.
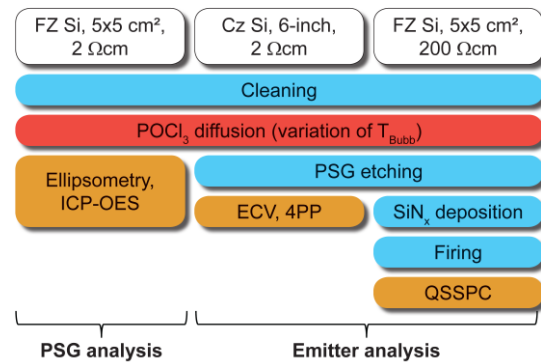
Figure 1: Sample preparation for PSG and emitter characterization. For POCl₃ diffusion, several bubbler temperatures (T_Bubb) were used.

After a wet-chemical cleaning procedure, 60 wafers are placed in the quartz boat of a commercial diffusion furnace from Centrotherm. In this experiment, we adjust a bubbler temperature ranging from 15.5°C to 24.5°C. After each POCl₃ diffusion process, the PSG layer is characterized by its thickness, determined by spectroscopic ellipsometry and the total amount of phosphorus (P dose), determined by Inductively Coupled

Plasma Optical Emission Spectrometry (ICP-OES) using the 2 Ωcm FZ samples. The emitter analysis is performed after the PSG removal. The sheet resistance for each wafer is determined by mapping (5x5 measuring points on 6-inch Cz), using a Four-Point-Prober (4PP). Additionally, for all diffusions the sheet resistance from wafers at different slot positions in the quartz boat is measured. The active doping profile is measured by an Electrochemical Capacitance-Voltage profiler (ECV). For evaluation of the emitter saturation current density (j_{0E}) from Quasi Steady State Photo-Conductance decay (QSSPC) measurements in high-injection conditions [6], the 200 Ωcm FZ wafers were passivated on both sides with silicon nitride (SiN_x) by PECVD and co-fired in a commercial belt furnace.

3   RESULTS

3.1 Analysis of the PSG layer

First of all, we analyse the PSG thickness by spectroscopic ellipsometry. It should be noted that the measured thickness includes the PSG growth during the drive-in step, due to a high oxygen flow. In Fig. 2 PSG thickness is shown in dependence of the bubbler temperature. The difference in PSG thickness between lowest and highest bubbler temperature is only about 4 nm. The PSG thickness increases approximately parabolic with bubbler temperature, as already shown for the $POCl_3$-N_2 gas flow variation [7].
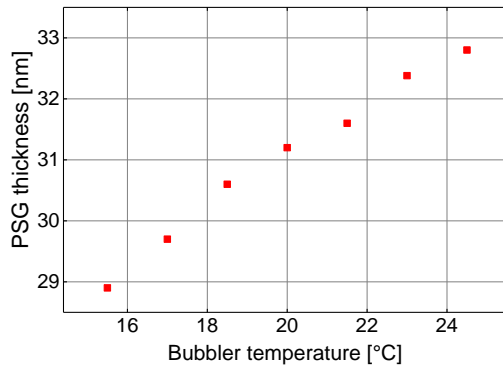
Figure 2: PSG thickness in dependence of bubbler temperature, measured with spectroscopic ellipsometry.
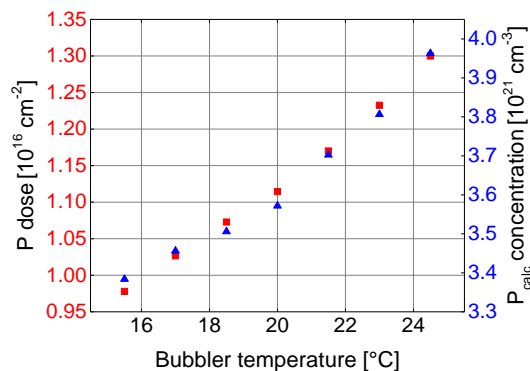
Figure 3: P dose in the PSG (left y-axis), measured with ICP-OES and calculated lower limit for P concentration in the PSG (right y-axis) as a function of $POCl_3$ bubbler temperature.

In Fig. 3, the measured P dose (left y-axis) is shown in dependence of bubbler temperature. In a first approximation, a linear relation between P dose and bubbler temperature is observed, which is analogous to a $POCl_3$-N_2 gas flow variation [8].

An average phosphorus concentration in the PSG can be determined by dividing the measured P dose by the PSG thickness. In should be noted that the PSG is probably a multilayer system [9], including a SiO_2 layer next to the Si-interface, where the P concentration might be reduced. As already mentioned, the PSG thickness increases also slightly due to the drive-in step. Therefore, the calculated P concentration in the PSG should be expected to be a lower limit [8]. The determined P concentration in the PSG for the standard bubbler temperature of 20°C is about $3.6 \cdot 10^{21}$ cm^{-3}. In comparison to [8], this determined value is less than half, which can be explained by the missing drive-in step in [8].

3.2 Analysis of the emitter

Fig. 4 shows the active doping profile of the emitter in dependence of bubbler temperature. A higher bubbler temperature clearly changes the plateau depth, while the tail region remains almost unchanged. The maximum concentration of active P next to the surface is 3-$4 \cdot 10^{20}$ cm^{-3}, but the total P concentration is expected to be much higher due to inactive phosphorus [4].
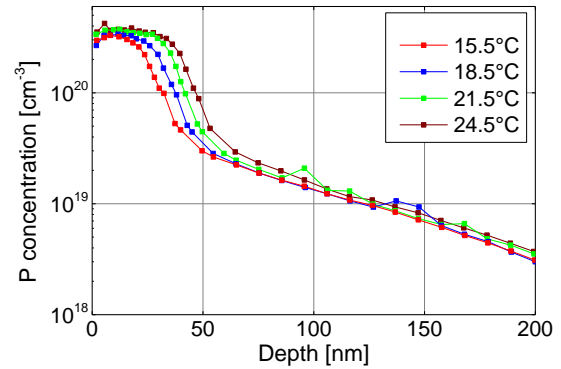
Figure 4: Emitter profiles in dependence of bubbler temperature, measured with ECV. The measurement was performed in the center of the wafer.
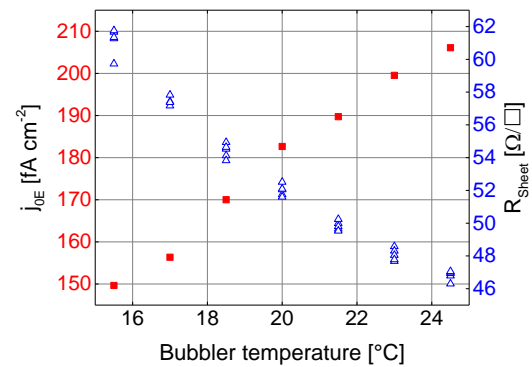
Figure 5: The emitter saturation current density (left y-axis) in dependence on the bubbler temperature, measured with QSSPC at an injection density of $1.5 \cdot 10^{16}$ cm^{-3}. The sheet resistance (right y-axis), is measured with 4PP for different bubbler temperatures.

The emitter saturation current density (left y-axis), measured by QSSPC, is shown in Fig. 5. The specified injection carrier density for evaluation is $1.5 \cdot 10^{16}$ cm^{-3}. A similar trend can be observed as for the PSG thickness. The electrical losses of the emitter can be reduced by using a lower bubbler temperature, which is also investigated for solar cell production in the next chapter. The right y-axis of Fig. 5 shows sheet resistance (R_{Sheet}) with respect to the slot position in the quartz boat during the diffusion process (slots: 10, 20, 30, 40 and 50). A very good homogeneity over the tube length is demonstrated.
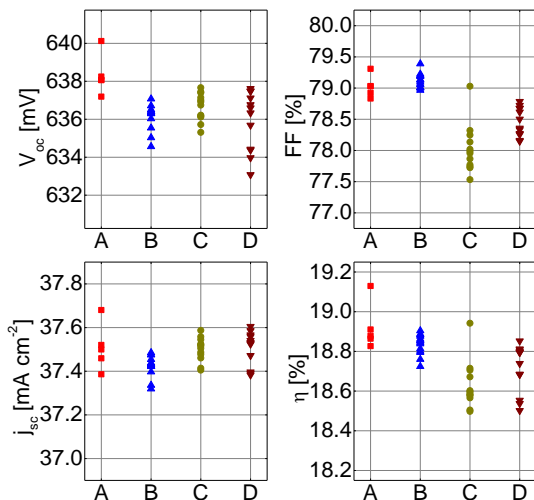
3.3 Effect on solar cells

Finally, we investigated the effect of bubbler temperature on industrial screen-printed 6-inch p-type Cz solar cells with full area Al-BSF. Therefore, four different emitters have been chosen with diffusion parameters given in Table I. The IV data (measured with a commercial IV flasher) is shown in Fig. 6.

Table I: Four different emitter groups, in dependence of POCl$_3$-N$_2$ gas flow (Φ_{POCl3}) and bubbler temperature.

Group	Φ_{POCl3} [a.u.]	T_{Bubb} [°C]	R_{Sheet} [Ω/sq]
A	Φ_0	20	63.2
B	$1.33\ \Phi_0$	15.5	61.1
C	$0.87\ \Phi_0$	20	69.3
D	Φ_0	18.5	66.9

Emitter A is the reference process with the POCl$_3$-N$_2$ gas flow of Φ_0 and a bubbler temperature of 20°C. Emitter B has a similar sheet resistance, but was obtained by increasing the POCl$_3$-N$_2$ gas flow and reducing the bubbler temperature at the same time. In comparison to the reference, group B has in average a slightly higher fill factor (FF), which is caused by a lower sheet resistance. On the other hand, group B has a reduced open circuit voltage (V_{oc}), which can be explained by increased SRH recombination due to higher inactive phosphorus concentration.

For group C the POCl$_3$-N$_2$ gas flow is decreased, while the bubbler temperature is unchanged. In comparison to the reference, the fill factor is lower by 1%$_{abs}$ due to the higher sheet resistance and less phosphorus precipitation. At the same time, also V_{oc} is lower, which can be explained by an increase of the saturation current density of the first diode (two diode model was fitted). For group D, the bubbler temperature is reduced, while POCl$_3$-N$_2$ gas flow is unchanged. The effect on V_{oc} and FF is similar as in group C.

4 CONCLUSIONS AND OUTLOOK

We investigated systematically the influence of the bubbler temperature on PSG and emitter formation. The PSG was characterised by its thickness and P dose. By combining these two results, we determined a lower limit for the P concentration in the PSG of $3.6 \cdot 10^{21}$ cm^{-3} ($T_{Bubb} = 20$°C). On the other hand, we characterized the emitter by the active doping profile. The plateau depth is clearly dependent on bubbler temperature. In addition, we examined the influence on emitter saturation current density and fabricated 6-inch solar cells with the novel diffusion parameters.

This investigation encourages the general under-standing of PSG and emitter formation. Further, the experimental data helps to improve existing phosphorus diffusion models by including the PSG properties. This work also showed that during POCl$_3$ diffusion processes more sensitive parameters can be adjusted to achieve emitter structures with increased electrical performance.

5 ACKNOWLEDGEMENTS

Figure 6: IV measurement: Emitter A is our reference with POCl$_3$-N$_2$ gas flow of Φ_0 and bubbler temperature of 20°C. Emitter B has a similar sheet resistance, by increasing POCl$_3$-N$_2$ gas flow and reducing bubbler temperature at the same time. For emitter C POCl$_3$-N$_2$ gas flow is reduced, while for emitter D bubbler temperature is reduced.

6 REFERENCES

[1] S.T. Dunham, J. Electrochem. Soc. 139 (1992) 2628.
[2] H. Bracht, H.H. Silvestri, I.D. Sharp, E.E. Haller, Phys. Rev. B 75 (2007) 035211.
[3] H. Wagner, A. Dastgheib-Shirazi, R. Chen, S.T. Dunham, M. Kessler, P.P. Altermatt, Proc. 37th IEEE PVSC, Seattle 2011, 2957.
[4] A. Dastgheib-Shirazi, M. Steyer, G. Micard, H. Wagner, P.P. Altermatt, G. Hahn, Proc. 38th IEEE PVSC, Austin 2012, 1584.
[5] J. Schön, W. Warta, Proc. 23rd EU PVSEC, Valencia 2008, 1851.
[6] D.E. Kane, R.M. Swanson, Proc. 18th IEEE PVSC, Las Vegas 1985, 578.
[7] J.M. Eldridge, P. Balk. Transactions of the Metallurgical Society of AIME, 242 (1968) 539.
[8] M. Steyer, A. Dastgheib-Shirazi, H. Wagner, G. Micard, P.P. Altermatt, G. Hahn, Proc. 27th EU PVSEC, Frankfurt 2012, 1325.
[9] R.N. Ghoshtagore, Thin Solid Films, 25(2) (1975) 501.